An improved friction calculation for water level and flow velocity simulation

Yiqun Sun, Weimin Bao, Liping Zhao, Xiaoqiang Yang, Boliang Ding, Hao Wang, Lin Hu and Peng Jiang

ABSTRACT

Flow friction is the key to studying water movement and has been one of the most important research topics in hydraulics and river dynamics. The roughness coefficient in the Manning formula represents friction applied to the flow by channel and changes with the river section characteristics, water level, and flow velocity. However, the Manning formula tends to simulate the friction with little variability, which contributes to large errors in the simulation of water level and flow velocity. To solve this problem, we proposed an improved friction formula based on the relationships between roughness coefficient and energy gradient and developed a differential model of one-dimensional flow with the proposed friction formula. The developed model was tested against both the experimental flood data and observed flow data in Qiantang River, China. The results indicated that the proposed friction formula provides a better simulation of target friction than the original Manning friction formula. The parameters in the proposed friction formula are less sensitive to the river section characteristics. Our results also showed that the developed differential model using the proposed friction formula can simulate the water level and flow velocity well in both the calibration and validation period and can improve the simulation of water level in tidal reach.

Key words | energy gradient, flood, friction, improved friction formula, Qiantang River

Yiqun Sun
Weimin Bao
Liping Zhao
Lin Hu
Peng Jiang (corresponding author)
State Key Laboratory of Hydrology-Water Resources and Hydraulic Engineering,
Hohai University,
Nanjing 210098,
China
E-mail: *peng.jiang.j@gmail.com*

Yiqun Sun
Weimin Bao
Lin Hu
Peng Jiang
College of Hydrology and Water Resources,
Hohai University,
Nanjing 210098,
China

Liping Zhao
Research Center on Flood and Drought Disaster Reduction of the Ministry of Water Resources,
China Institute of Water Resources and Hydropower Research,
Beijing 100038,
China

Xiaoqiang Yang
Department of Aquatic Ecosystem Analysis and Management,
Helmholtz Centre for Environmental Research-UFZ,
Magdeburg 39114,
Germany

Boliang Ding
Hao Wang
Hydrological Bureau of Zhejiang Province,
Hangzhou 310009,
China

INTRODUCTION

Flow friction is the key to understanding water movement. In either the Navier–Stokes equations or the Saint–Venant equations, the structure of the friction formula is empirically based, which may cause significant errors in real application. As a result, hydraulic friction or friction loss has been one of the most important research topics in hydraulics and river dynamics (Jones 1976; Bathurst 1985). Research on this topic has focused on: (1) the development of the flow resistance formula under the condition of fixed bed, including the Chezy formula (Herschel 1897), Du Buat formula (Du Buat 1822), Eytelwein formula (Eytelwein 1826), Darcy–Weisbach formula (Chow *et al.* 1988), Darcy–Bazin formula (Darcy & Bazin 1865), Manning formula (Willcocks & Holt 1899), etc.; (2) the roughness research under the conditions of turbid water-movable bed (Dou 1982; Grant & Madsen 1982; Zhao & Zhang 1997). However, the complex

doi: 10.2166/nh.2019.039

mechanism behind the friction has not been comprehensively investigated.

The Manning formula is the common expression of friction in the channel flow:

$$u = \frac{1}{n} R^{2/3} S^{1/2} \tag{1}$$

where u is the mean velocity at a cross-section (m/s), R is hydraulic radius (m), n is roughness coefficient ($s/m^{1/3}$), S is the gradient. We define f_m ($f_m = gS$) as the friction calculated by the Manning formula (m/s^2):

$$f_m = gn^2 \frac{|u|u}{R^{4/3}} \tag{2}$$

where g is acceleration of gravity (m/s^2). This formula reflects that the friction is proportional to u^2, and inversely proportional to $R^{4/3}$. The roughness coefficient factor usually varies with the characteristic of river section, water level, flow velocity, etc. (De Doncker *et al.* 2009).

As one of the parameters in flood calculation, the roughness of a natural river is determined by the roughness degree of the riverbed and quay wall, shape of river section, state of flow, sediment concentration, etc. (Limerinos 1970; Arcement & Schneider 1989; Xiekang *et al.* 2000). Some common methods for the estimation of roughness include using empirical formulae or charts, hydraulic methods, roughness inverse techniques (Khatibi *et al.* 2000; Dong & Yang 2002; Yen 2002), roughness curves (Khatibi *et al.* 2000), and the comprehensive roughness method (Yang *et al.* 2007). Bao *et al.* (2009) examined the impact of roughness on the water level of the tidal reach and separated the roughness into floodplain roughness and main channel roughness in cross-sections with obvious floodplain. Their results indicate that the changes of roughness have a great impact on water level calculation. The floodplain water level is dominated by the floodplain roughness while the low water level is mainly affected by the main channel roughness (Bao *et al.* 2010). Based on these findings, the relationship between roughness and water level was proposed (Bao *et al.* 2009).

More and more studies have indicated that flow energy plays an important role in the study of flow law. The energy equation has been widely applied in various research topics including energy dissipation of bend flow (Li & Fang 2010), sediment movement (Yang 1972; McLaren & Bowles 1985), study of river meandering mechanism (Ikeda *et al.* 1981; Nanson & Knighton 1996; Yao *et al.* 2010), numerical modeling on 1D river flow (Murillo & García-Navarro 2014), correlation between the flow energy loss and the channel deposition and erosion (Qi *et al.* 2013), and numerical modeling of flow resistance (Pannone *et al.* 2013). These studies examined the correlations between flow energy and flow motion law as well as riverbed friction. However, they did not apply the differential energy gradient frictional resistance formula in flow motion equation, or use it in practice.

In this study, we strive to investigate the relationship between roughness and the energy gradient change to: (1) examine the changing characteristics of friction during flood processes; (2) develop a function for roughness and energy gradient and propose an improved friction formula of one-dimensional flow; and (3) evaluate the proposed friction formula with the flow data from both experiments and a case study in Qiantang River.

DATA

Experiment setup and flood data collection

The flood experiment was conducted in an open flume in the hydraulics laboratory of Hohai University. The slope of the glass rectangular flume could be adjusted upon request. The flume was 7.73 m in length and 0.31 m in width. Three sections were set up to measure the water level and flow velocity (Figure 1). The friction between two sections is related to the flume slope, boundary roughness, flow characteristics, and aquatic plants, etc. During the experiment, the riverbed roughness, sectional shape, and the slope were kept unchanged. The changes of friction and energy were investigated under different discharges (reflecting different flow characteristics) and different densities of aquatic plants (reflecting the aquatic plant factor). The intake pump of the flume was equipped with a flow meter with measured accuracy at 2.8×10^{-6} m^3/s. Discharge could be adjusted by the rotary switch in the intake valve. The maximum discharge of the intake pump was 0.0283 m^3/s. The aquatic plant factors can be controlled by different quantities and densities of the branch fences in the flume. Eleven densities

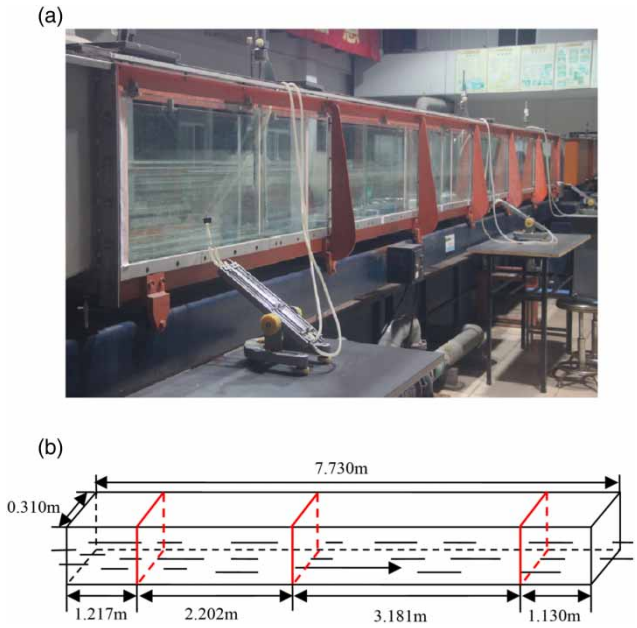

Figure 1 | Flood simulator. (a) picture of experimental installation; (b) diagram of experimental installation.

of fence branches were used in the experiment. Letters a–k represent different densities of each fence branches (a: lowest density; k: highest density). Twelve types of fence were set up with different fence combinations. The fence combination at each position is presented in Table 1. The experiment was conducted in two steps. First, the relationship between water level and discharge under different conditions of water plant was investigated. In this situation, the slope and channel characteristics were the same and there was no backwater effect, the relationship between water level and discharge was only related to the type of fence. For 12 types of fence and three sections (upper, middle and lower), 36 stage-discharge relationships were obtained and used for calculating the flood process in the second step. In the second step, flood data was collected. For each type of fence, four floods were simulated. The peak water level, peak time and period number of 48 floods are shown in Table 2.

Table 1 | Fence setup in lab experiment

	Fence setting position					
Type of fence	**1#**	**2#**	**3#**	**4#**	**5#**	**6#**
1			d			
2			i			
3	d		i			
4	d	f	i			
5	d	f	j	b		a
6	c;d	g	j	e		a
7	d	e;f	j	b	h	a
8	c;d	g	i;j	b	h	a
9	d;k	e;f	j	b	h	a
10	d;k	e;f;g	j	b	h	a
11	d;k	e;f;g	i;j	b	h	a
12	c;d;k	e;f;g	i;j	b	h	a

River section and data

The observed data in Zhijiang hydrologic station (water level and discharge) and Wenjiayan water level station (water level) were collected for the validation and assessment of the proposed friction formula. Doppler ultrasonic wave equipment was set up in Zhijiang hydrologic station for accurate measurements. The distance between the two stations was 616 m. There was no tributary in this river reach so that no lateral inflow would contribute to the streamflow during non-rainy period.

METHODS

Ideal friction calculation

The ideal friction calculation is derived from the Saint–Venant equation. As a result, the basic assumption of the ideal friction calculation is that the Saint–Venant equation could describe the unsteady flow of an open channel. The one-dimensional flow motion equation expressed with section average flow velocity u (m/s) and water level z (m) can be written as Equation (3). The effect of the bed slope is considered in item $\frac{\partial z}{\partial x}$, which could be expressed as $g\left(\frac{\partial h}{\partial x} - i\right)$:

$$\frac{\partial u}{\partial t} + u\frac{\partial u}{\partial x} + g\frac{\partial z}{\partial x} + f = 0 \tag{3}$$

$$f = -\frac{\partial u}{\partial t} - u\frac{\partial u}{\partial x} - g\left(\frac{\partial h}{\partial x} - i\right) \tag{4}$$

Table 2 | Sampling statistics of 48 floods

	Upper section		Middle section		Lower section		
Flood no.	Peak water level (m)	Peak time (s)	Peak water level (m)	Peak time (s)	Peak water level (m)	Peak time (s)	Period number
1-1	0.1773	88	0.1725	88	0.1685	96	46
1-2	0.1523	60	0.1455	56	0.1445	56	30
1-3	0.1338	56	0.1305	64	0.1270	52	34
1-4	0.1068	52	0.1025	52	0.1020	52	33
2-1	0.1833	84	0.1775	84	0.1700	76	43
2-2	0.1613	64	0.1565	68	0.1510	72	38
2-3	0.1383	60	0.1325	60	0.1265	64	32
2-4	0.1168	60	0.1135	56	0.1025	60	30
3-1	0.1858	68	0.1750	68	0.1690	72	34
3-2	0.1663	68	0.1575	68	0.1470	68	35
3-3	0.1426	60	0.1335	56	0.1255	60	25
3-4	0.1248	56	0.1155	56	0.1050	64	25
4-1	0.1868	64	0.1695	60	0.1640	64	34
4-2	0.1653	64	0.1455	60	0.1405	56	31
4-3	0.1378	64	0.1245	64	0.1155	68	30
4-4	0.1218	56	0.1095	56	0.0980	60	23
5-1	0.2003	88	0.1855	88	0.1630	84	46
5-2	0.1708	72	0.1555	80	0.1440	72	36
5-3	0.1458	64	0.1325	68	0.1195	64	30
5-4	0.1213	52	0.1095	52	0.1005	56	25
6-1	0.2058	64	0.1815	64	0.1645	64	44
6-2	0.1828	76	0.1575	76	0.1450	76	47
6-3	0.1518	56	0.1245	56	0.1150	60	34
6-4	0.1358	72	0.1085	68	0.1020	68	36
7-1	0.2098	88	0.1915	96	0.1655	76	44
7-2	0.1838	80	0.1695	80	0.1455	84	41
7-3	0.1563	60	0.1435	64	0.1230	64	38
7-4	0.1343	56	0.1225	52	0.1030	60	32
8-1	0.2233	72	0.1985	76	0.1675	80	48
8-2	0.1978	68	0.1735	72	0.1455	80	41
8-3	0.1773	64	0.1555	64	0.1285	68	37
8-4	0.1438	56	0.1265	60	0.0990	56	34
9-1	0.2228	80	0.1935	84	0.166	84	52
9-2	0.1928	76	0.1645	76	0.1405	76	43
9-3	0.1623	68	0.1395	72	0.1170	80	39
9-4	0.1403	68	0.1195	68	0.1030	68	37
10-1	0.2318	80	0.1955	84	0.1695	96	53
10-2	0.2008	76	0.1715	76	0.1445	84	43

(*continued*)

Table 2 | continued

	Upper section		Middle section		Lower section		
Flood no.	Peak water level (m)	Peak time (s)	Peak water level (m)	Peak time (s)	Peak water level (m)	Peak time (s)	Period number
10-3	0.1733	60	0.1425	68	0.1215	60	38
10-4	0.1448	52	0.1185	60	0.1000	56	34
11-1	0.2353	76	0.2015	84	0.1670	76	55
11-2	0.2043	76	0.1725	80	0.1415	88	50
11-3	0.1833	64	0.1555	64	0.1265	68	40
11-4	0.1483	56	0.1255	56	0.0995	60	33
12-1	0.2353	72	0.1985	72	0.1650	84	55
12-2	0.2138	72	0.1785	72	0.1485	72	42
12-3	0.1743	64	0.1445	68	0.1190	68	38
12-4	0.1523	56	0.1245	56	0.0980	64	34

where f is friction, z is the waterhead, h is the flow depth, i is the bed slope, and g is gravitational acceleration. The most ideal friction formula can be expressed as Equation (4). Hence, the differential expression of the ideal friction with the Pressiman differential scheme weighted by θ can be written as:

$$\overline{f^{i,i+1}_{j,j+1}} = -\left(\frac{\Delta u_{j+1}+\Delta u_j}{2\Delta t}+\frac{\theta}{\Delta x}(u^i_{j+1}\Delta u_{j+1}-u^i_j\Delta u_j) + \frac{u^{i2}_{j+1}-u^{i2}_j}{2\Delta x}+\frac{g\theta}{\Delta x}(\Delta z_{j+1}-\Delta z_j)+g\frac{z^i_{j+1}-z^i_j}{\Delta x}\right) \quad (5)$$

where $\Delta u_k = u^{i+1}_k - u^i_k$, $\Delta z_k = z^{i+1}_k - z^i_k$, $k = j, j+1, i$ is time t, j is position, $i+1$ is the next time step(Δt), and $j+1$ is the next position step(Δx).

Any proposed friction formula should be evaluated based on the goodness of fit between simulated friction and ideal friction (Equations (4) and (5)). In this paper, the ideal friction was used as the target friction for evaluation.

Manning friction calculation

The differential form of the Manning friction formula (Equation (2)) with the Pressiman differential scheme weighted by θ can be written as:

$$\overline{(f_m)^{i,i+1}_{j,j+1}} = gn^2\left(\frac{\theta u^i_{j+1}}{(R^i_{j+1})^{\frac{4}{3}}}\Delta u_{j+1}+\frac{\theta u^i_j}{(R^i_j)^{\frac{4}{3}}}\Delta u_j-\frac{\theta u^{i2}_{j+1}}{2(R^i_{j+1})^{\frac{7}{3}}}\Delta h_{j+1} - \frac{\theta u^{i2}_j}{2(R^i_j)^{\frac{7}{3}}}\Delta h_j+\frac{u^{i2}_{j+1}}{2(R^i_{j+1})^{\frac{4}{3}}}+\frac{u^{i2}_j}{2(R^i_j)^{\frac{4}{3}}}\right) \quad (6)$$

$\overline{f_m\, j,j+1^{\,i,i+1}}$ represents the mean value between the reach section $[j,\ j+1]$ and period $[i,\ i+1]$. For the experimental floods, the flow velocity, water level (or water depth) of the upper and lower sections $[j,\ j+1]$ are all available for the calculation of both ideal friction and Manning friction values with Equations (5) and (6).

Changes of friction during flood processes

The structure of the friction formula could be evaluated with simulated friction changes during flood processes. Figure 2 shows the changes of ideal friction and Manning friction with changes of water level. The target friction increases rapidly at the beginning of a flood and then shows a sharp decrease before the flood peak appears. It reaches its minimum value around the flood peak. Changes of target friction are determined by spatiotemporal variation of flow velocity and surface slope. There are multiple peaks during the water rising and recession period. Manning friction is relatively larger when the water level is low (water rising and recession period) as the hydraulic radius is smaller during low water level periods than that during flood peak periods. Manning friction is proportional to flow velocity (u^2) and is inversely proportional to hydraulic radius ($R^{4/3}$). However, the hydraulic radius changes in the same direction with flow velocity, thus the synchronization between flow velocity and hydraulic radius often has an offset effect on

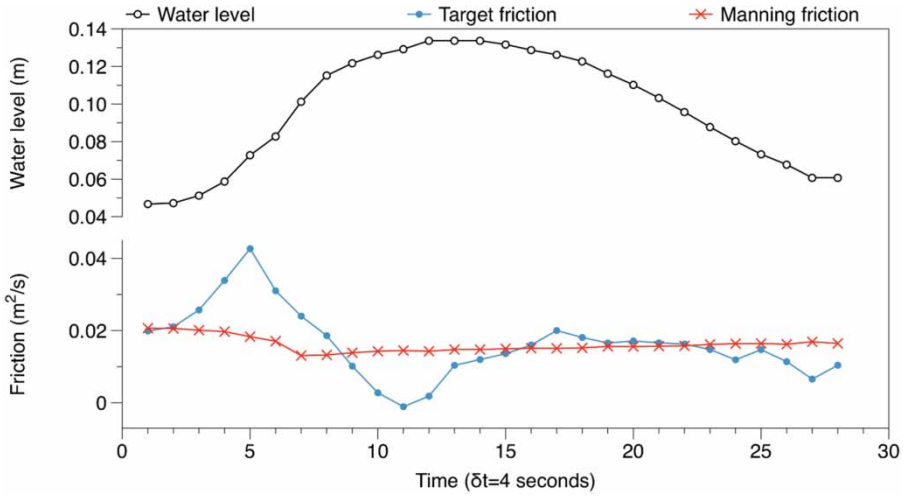

Figure 2 | Changes of target friction and Manning friction with water level during a flood (Flood 1-2).

Manning friction, which explains the smaller variation of Manning friction compared to target friction. The small correlation coefficient (0.2055) indicates the inconsistency between changes of target friction and Manning friction.

Changes of Manning roughness coefficient during flood processes

Based on the analyses, the constant Manning roughness coefficient may introduce large errors to Manning friction estimation. As a result, understanding how the roughness coefficient changes during a flood is the key to improving the calculation of Manning friction. For every time step we can change the roughness coefficient to make the Manning friction and target friction equal. In this situation, the time-varying roughness coefficient can be expressed as:

$$\overline{(n^2)_{jj+1}^{i,i+1}} = -\frac{\dfrac{\Delta u_{j+1}+\Delta u_j}{2\Delta t}+\dfrac{\theta}{\Delta x}\left(u_{j+1}^{i}\Delta u_{j+1}-u_j^{i}\Delta u_j\right)+\dfrac{u_{j+1}^{i2}-u_j^{i2}}{2\Delta x}+\dfrac{g\theta}{\Delta x}\left(\Delta z_{j+1}-\Delta z_j\right)+g\dfrac{z_{j+1}^{i}-z_j^{i}}{\Delta x}}{g\left(\dfrac{\theta u_{j+1}^{i}}{(R_{j+1}^{i})^{\frac{4}{3}}}\Delta u_{j+1}+\dfrac{\theta u_j^{i}}{(R_j^{i})^{\frac{4}{3}}}\Delta u_j-\dfrac{\theta u_{j+1}^{i2}}{2(R_{j+1}^{i})^{\frac{7}{3}}}\Delta h_{j+1}-\dfrac{\theta u_j^{i2}}{2(R_j^{i})^{\frac{7}{3}}}\Delta h_j+\dfrac{u_{j+1}^{i2}}{2(R_{j+1}^{i})^{\frac{4}{3}}}+\dfrac{u_j^{i2}}{2(R_j^{i})^{\frac{4}{3}}}\right)} \tag{7}$$

The total energy (S) of the flow in the channel section is expressed as:

$$S = z+\frac{\alpha u^2}{2g} \tag{8}$$

To investigate the relation between roughness coefficient and energy gradient, we calculated the energy gradient using a Pressiman differential scheme weighted by θ as below:

$$\overline{(s_e)_{j,j+1}^{i,i+1}} = \frac{\theta\alpha}{g\Delta x}\left(u_{j+1}^{i}\Delta u_{j+1}-u_j^{i}\Delta u_j\right)+\frac{\alpha(u_{j+1}^{i2}-u_j^{i2})}{2g\Delta x}+\frac{\theta}{\Delta x}\left(\Delta z_{j+1}-\Delta z_j\right)+\frac{z_{j+1}^{i}-z_j^{i}}{\Delta x} \tag{9}$$

where S_e is the energy gradient and α is the proportional coefficient between the kinetic energy of the mean velocity in the section and point velocity. Figure 3 shows the changes of Manning roughness coefficient, water level, flow velocity, and energy gradient during a flood (Flood 1-2). Manning roughness coefficient exhibits a poor correlation with both water level and flow velocity. However, it shows a high negative correlation with energy gradient (–0.7674). To confirm the correlation between the Manning roughness coefficient and energy gradient, we calculated the correlation coefficient between them for 48 floods as listed in

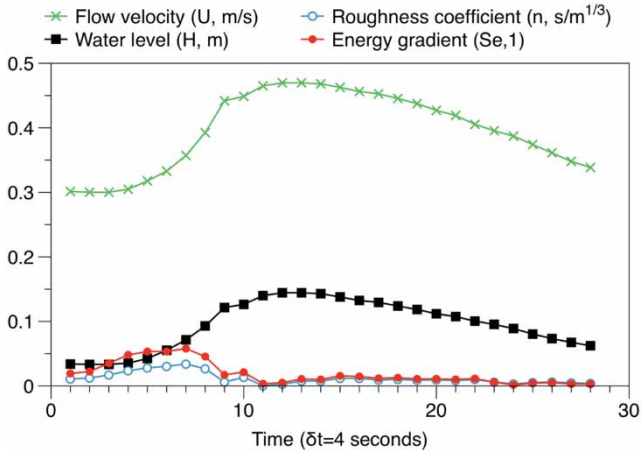

Figure 3 | Change process of *n*, *U*, *H* and *Se* during Flood 1–2.

Table 3. Among the three examined flood factors, the energy gradient exhibits the highest average correlation coefficient (–0.871) with Manning roughness coefficient.

Friction formula and dynamic differential model based on energy-gradient-dependent roughness coefficient

Manning roughness coefficient and energy gradient for each time step in Flood 1-2 are plotted in Figure 4, which shows an approximately linear relationship. We assume that the linear relationship between them can be expressed as:

$$\overline{(n_r)_{j,j+1}^{i,i+1}} = n_0 - \alpha_f \overline{(s_e)_{j,j+1}^{i,i+1}} \tag{10}$$

Table 3 | Correlation coefficients between roughness and water level, flow velocity and energy gradient

Flood number	C_h	C_u	C_{se}	Flood number	C_h	C_u	C_{se}
1-1	−0.0368	0.0007	−0.796	7-1	0.6252	0.0068	−0.9221
1-2	−0.0466	0.0049	−0.7674	7-2	0.6406	0.0055	−0.8988
1-3	−0.0228	0.0049	−0.5728	7-3	0.5876	0.0039	−0.8911
1-4	0.1321	0.0107	−0.7439	7-4	0.6849	0.0036	−0.8104
2-1	−0.2156	−0.0136	−0.8388	8-1	0.5546	0.0048	−0.9472
2-2	−0.0859	−0.0024	−0.7775	8-2	0.6864	0.0052	−0.9132
2-3	0.0375	0.0022	−0.7829	8-3	0.7248	0.0045	−0.9044
2-4	0.0755	0.0024	−0.7584	8-4	0.7438	0.0033	−0.8305
3-1	−0.0325	0.0003	−0.8263	9-1	0.7088	0.0056	−0.9280
3-2	0.0480	0.0025	−0.8566	9-2	0.7420	0.0048	−0.9128
3-3	0.0450	0.0019	−0.8705	9-3	0.6583	0.0037	−0.9347
3-4	0.2143	0.0041	−0.7938	9-4	0.7690	0.0030	−0.8420
4-1	0.1691	0.0049	−0.8913	10-1	0.6457	0.0047	−0.9494
4-2	0.1039	0.0027	−0.8714	10-2	0.6694	0.0041	−0.9321
4-3	0.2358	0.0037	−0.7980	10-3	0.7318	0.0035	−0.9095
4-4	0.3390	0.0035	−0.7129	10-4	0.7932	0.0029	−0.8775
5-1	0.4386	0.0068	−0.7658	11-1	0.5721	0.0042	−0.8973
5-2	0.2924	0.0041	−0.9271	11-2	0.4487	0.0025	−0.957
5-3	0.4044	0.0044	−0.8139	11-3	0.5589	0.0029	−0.8877
5-4	0.3993	0.0032	−0.7588	11-4	0.6697	0.0026	−0.8259
6-1	0.3366	0.0047	−0.8743	12-1	0.4470	0.0028	−0.8965
6-2	0.2929	0.0032	−0.9372	12-2	0.5012	0.0027	−0.8729
6-3	0.5359	0.005	−0.8361	12-3	0.5047	0.0021	−0.8452
6-4	0.5731	0.0042	−0.7349	12-4	0.5174	0.0019	−0.7882

Note: C_h, C_u, and C_{Se} represent the correlation coefficient between the roughness coefficient and water depth, flow velocity and energy gradient, respectively.

Then the differential form of the relationship between the roughness coefficient and energy gradient can be written as:

$$n_r = n_0 - \alpha_f \frac{\partial}{\partial x}\left(z + \frac{\alpha u^2}{2g}\right) \tag{11}$$

The improved Manning formula f_{mr} can be expressed as:

$$f_{mr} = \left(n_0 - \alpha_f \frac{\partial}{\partial x}\left(z + \frac{\alpha u^2}{2g}\right)\right) g \frac{|u|u}{R^{\frac{4}{3}}} \tag{12}$$

where n_0 is a constant coefficient ($s^2/m^{2/3}$), α_f is the proportional coefficient of frictional resistance variation caused by energy variation ($s^2/m^{2/3}$), f_{mr} is the friction calculated by Manning formula (m/s^2), and n_r is the roughness coefficient

Without lateral inflow, the continuity equation expressed with water depth h (m) and flow velocity u (m/s) can be written as:

$$\frac{\partial h}{\partial t} + u\frac{\partial h}{\partial x} + h\frac{\partial u}{\partial x} = 0 \tag{13}$$

Therefore, Equations (3), (12) and (13) constitute the improved hydrodynamic model, and the differential form with Pressiman difference scheme (Bao *et al.* 2009) can be expressed as:

$$\begin{aligned} &a_1\Delta u_{j+1} + a_2\Delta u_j + a_3\Delta h_{j+1} + a_4\Delta h_j = a_0 \\ &b_{r1}\Delta u_{j+1} + b_{r2}\Delta u_j + b_{r3}\Delta h_{j+1} + b_{r4}\Delta h_j = b_{r0} \end{aligned} \tag{14}$$

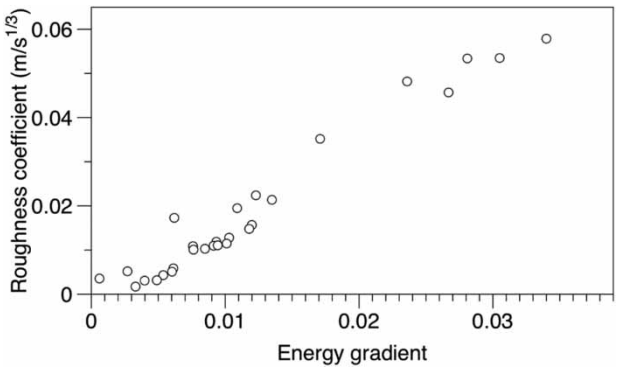

Figure 4 | Relation between the roughness coefficient and energy gradient.

where:

$$\begin{aligned}
a_1 &= \frac{\theta}{\Delta x}h^i_{j+1},\ a_2 = \frac{\theta}{\Delta x}h^i_j,\ a_3 = \frac{1}{2\Delta t} + \frac{\theta}{\Delta x}u^i_{j+1},\ a_4 = \frac{1}{2\Delta t} \\
&- \frac{\theta}{\Delta x}u^i_j,\ a_0 = -\frac{1}{\Delta x}(u^i_{j+1}h^i_{j+1} - u^i_j h^i_j) \\
b_{r1} &= \frac{1}{2\Delta t} + \frac{\theta}{\Delta x}u^i_{j+1} + \left(n_0\theta - \alpha_f\theta\frac{h^i_{j+1} - h^i_j}{\Delta x} - \frac{\alpha_f\alpha\theta}{g}\frac{u^{i2}_{j+1} - u^{i2}_j}{2\Delta x}\right) \\
&\frac{u^i_{j+1}}{(R^i_{j+1})^{4/3}} - \frac{\alpha_f\alpha\theta u^i_{j+1}}{2g\Delta x}\left(\frac{u^{i2}_{j+1}}{(R^i_{j+1})^{4/3}} + \frac{u^{i2}_j}{(R^i_j)^{4/3}}\right) \\
b_{r2} &= \frac{1}{2\Delta t} - \frac{\theta}{\Delta x}u^i_j + \left(n_0\theta - \alpha_f\theta\frac{h^i_{j+1} - h^i_j}{\Delta x} - \frac{\alpha_f\alpha\theta}{g}\frac{u^{i2}_{j+1} - u^{i2}_j}{2\Delta x}\right) \\
&\frac{u^i_j}{(R^i_j)^{4/3}} + \frac{\alpha_f\alpha\theta u^i_j}{2g\Delta x}\left(\frac{u^{i2}_{j+1}}{(R^i_{j+1})^{4/3}} + \frac{u^{i2}_j}{(R^i_j)^{4/3}}\right) \\
b_{r3} &= \frac{g\theta}{\Delta x} - \left(n_0\theta - \alpha_f\theta\frac{h^i_{j+1} - h^i_j}{\Delta x} - \frac{\alpha_f\alpha\theta}{g}\frac{u^{i2}_{j+1} - u^{i2}_j}{2\Delta x}\right)\frac{u^{i2}_{j+1}}{2(R^i_{j+1})^{7/3}} \\
&- \frac{\alpha_f\theta}{2\Delta x}\left(\frac{u^{i2}_{j+1}}{(R^i_{j+1})^{4/3}} + \frac{u^{i2}_j}{(R^i_j)^{4/3}}\right) \\
b_{r4} &= -\frac{g\theta}{\Delta x} - \left(n_0\theta - \alpha_f\theta\frac{h^i_{j+1} - h^i_j}{\Delta x} - \frac{\alpha_f\alpha\theta}{g}\frac{u^{i2}_{j+1} - u^{i2}_j}{2\Delta x}\right)\frac{u^{i2}_j}{2(R^i_j)^{7/3}} \\
&+ \frac{\alpha_f\theta}{2\Delta x}\left(\frac{u^{i2}_{j+1}}{(R^i_{j+1})^{4/3}} + \frac{u^{i2}_j}{(R^i_j)^{4/3}}\right) \\
b_{r0} &= gs_0 - \frac{u^{i2}_{j+1} - u^{i2}_j}{2\Delta x} - g\frac{h^i_{j+1} - h^i_j}{\Delta x} \\
&- \left(\frac{n_0}{2} - \alpha_f\frac{h^i_{j+1} - h^i_j}{\Delta x}s_0 - \frac{\alpha_f\alpha}{g}\frac{u^{i2}_{j+1} - u^{i2}_j}{2\Delta x}\right) \\
&\left(\frac{u^{i2}_{j+1}}{(R^i_{j+1})^{4/3}} + \frac{u^{i2}_j}{(R^i_j)^{4/3}}\right)
\end{aligned} \tag{15}$$

when $\alpha_f = 0$ and $n^2 = n_0$, Equation (15) is converted into the dynamic differential model with the Manning formula as friction.

RESULTS AND DISCUSSION

Experimental flood simulation with original Manning friction

Twelve types of fence represent 12 types of channel segment characteristics. To test the Manning friction formula for the

same reach, the parameter in the Manning formula under each type of fence was calibrated. For each fence module, three floods were used to calibrate parameter and one flood was used for validation. The simulation effect was evaluated by absolute relative error value (RE) using Equation (16):

$$RE(OB) = \left(1 - \frac{\sum_{i=1}^{L} |OB_i - OBC_i|}{\sum_{i=1}^{L} |OB_i|}\right) * 100\% \quad (16)$$

where OB and OBC are the observed and calculated variable values, respectively.

Table 4 shows the calibrated parameter (n^2) and the absolute relative error for both calibrated and validated floods. The low relative errors indicate poor simulation effects in both the calibration and the validation stage. The poor simulation was mainly due to the error introduced by the Manning friction. Figure 5 shows the comparison between the measured and calculated water level and flow velocity in the lower section. The differences between measured and calculated water level and flow velocity can be divided into three periods. (1) At the water rising period, the Manning friction was smaller than the target friction (Figure 2). Hence, the flow spread from the upper section to the lower section was much faster than the actual, which led to larger calculated water depth and smaller calculated flow velocity than the observed ones in the lower section. (2) Around the flood peak, the Manning friction is larger than the target friction (Figure 2) which leads to smaller calculated water depth and larger calculated flow velocity. (3) At the recession period, the calculated water level and flow velocity showed fluctuations around the measured water level and flow velocity because of the accumulated error during the calculation processes (Figure 5). The results of other floods showed similar characteristics, which indicates that the Manning friction calculation error may be the main reason for the calculated error of water depth and flow velocity.

Table 4 | Simulation results of water level (H) and flow velocity (U) by the Manning formula

Type of fence	n^2	RE(H)	RE(U)	Ver.RE(H)	Ver.RE(U)
1	0.0264	64.5	49.9	63.4	44.1
2	0.0314	66.8	38.7	67.5	53.6
3	0.0446	70.1	40.0	75.1	68.6
4	0.0411	72.3	63.8	68.6	54.3
5	0.0501	71.8	57.2	73.2	53.4
6	0.0595	74.2	63.5	74.1	63.9
7	0.0653	73.6	63.2	68.4	51.2
8	0.0669	76.1	69.2	73.3	64.4
9	0.0703	76.2	70.3	71.8	65.2
10	0.0716	75.5	69.9	72.9	65.6
11	0.0548	73.5	65.8	70.9	62.7
12	0.0630	73.5	49.3	69.9	16.8
Average	0.645	72.3	58.4	70.8	55.3

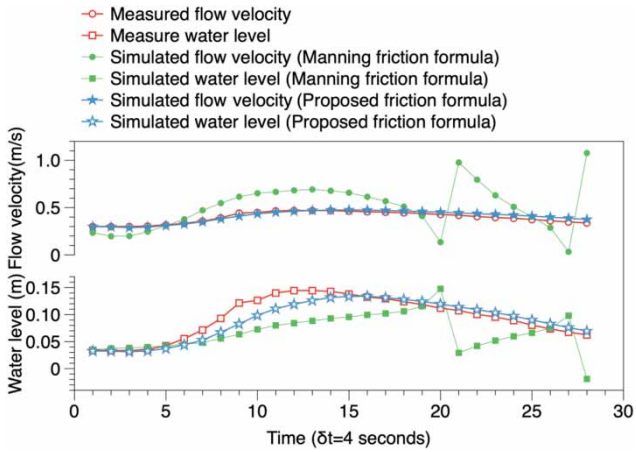

Figure 5 | Comparison of the measured and simulated water level and flow velocity by the Manning friction formula and proposed friction formula for Flood 1-2.

Experimental flood simulation with proposed friction formula

Roughness coefficient is considered to change with energy gradient in the proposed friction formula. It can be evaluated in two steps: (1) examine how well the proposed friction formula can simulate the target friction; (2) evaluate the ability of differential models with proposed friction formula to simulate the water depth and flow velocity. Table 5 shows the simulation results using the proposed friction formula. Table 5 indicates that the proposed friction formula can simulate the target friction well and the differential model driven by the proposed friction formula can simulate the water level and flow velocity well in both calibration and validation phases. The relative range of the

Table 5 | Simulation results of target friction (f), water level (H), and flow velocity (U) using the proposed friction formula

Type of fence	$n_0 \times 100$	α_f	RE(f)	RE(H)	RE(U)	Ver.RE(f)	Ver.RE(H)	Ver.RE(U)
1	–0.249	0.973	0.898	89.4	94.2	0.875	90.3	96.1
2	–0.318	0.973	0.820	92.6	95.0	0.779	92.6	96.2
3	–0.288	0.973	0.899	92.0	95.0	0.895	90.9	95.9
4	–0.339	0.973	0.922	91.9	96.3	0.907	89.9	96.7
5	–0.339	0.953	0.936	89.6	95.8	0.925	87.7	97.1
6	–0.336	0.937	0.917	89.1	94.7	0.908	86.2	94.6
7	–0.258	0.920	0.828	89.9	93.4	0.838	85.3	91.0
8	–0.225	0.913	0.856	89.6	92.3	0.863	86.5	90.9
9	–0.263	0.918	0.838	89.8	91.4	0.826	86.2	92.0
10	–0.173	0.909	0.859	89.2	92.5	0.872	84.7	91.0
11	–0.333	0.926	0.914	88.3	91.8	0.910	83.8	93.0
12	–0.339	0.931	0.765	90.8	93.0	0.763	86.6	95.0
Average	3.46	0.942	0.871	90.2	93.8	0.863	87.6	94.1

parameters in both Manning (n^2) and proposed friction formula (n_0, α_f) was also investigated for different fence types which represent different river section characteristics. The range of the parameters could be used to indicate the variability of the parameters for different river section characteristics.

The range for roughness factor n^2 in the Manning formula is:

$$V(n^2) = \frac{\max(n^2) - \min(n^2)}{mean\,(n^2)} * 100\% = \frac{0.0716 - 0.0264}{0.0538} = 84.0\%$$

The range of the parameters n_0 and α_f proposed friction formula are:

$$V(n_0) = \frac{0.00339 - 0.00173}{0.00288} = 57.6\%;$$
$$V(\alpha_f) = \frac{0.973 - 0.909}{0.942} = 6.8\%$$

Our results show that the parameters in the proposed friction formula are more stable than the parameters in the Manning friction formula. The range of the parameter α_f was only 6.8%, which means that this parameter is not sensitive to the changes of river section characteristics. Table 6 lists the simulation effect of the floods with the different types of fence using the proposed friction formula with the same parameter ($n_0 = -0.002146625$, $\alpha_f = 0.915392$). The good match between simulated and measured water level and flow velocity further confirms the generality of parameters in the proposed friction formula. To illustrate the simulation effect for a single flood, we selected Flood 1-2 for explanatory purposes. Figure 5 shows the comparison of the measured and simulated water level and flow velocity by the Manning friction formula and proposed friction formula for Flood 1-2. Figure 6 shows the comparisons among the target friction (f), the friction (f_{mr}) calculated by the proposed friction formula, and friction (f_m) calculated by the Manning formula. Figures 5 and 6 illustrate the improvement in simulating target friction, water level, and flow velocity with the proposed friction formula.

Table 6 | Simulation results of water level (H) and flow velocity (U) by the proposed friction formula with the same parameter for 12 types of fences[a]

Type of fence	1	2	3	4	5	6	7	8	9	10	11	12
RE(H)	84.5	87.7	86.2	86.4	85.8	85.5	85.9	85.3	85.5	85.1	83.4	86.0
RE(U)	91.1	93.5	93.2	93.2	92.9	92.9	91.0	90.4	90.9	90.4	91.4	93.0

[a]Parameters used in this simulation: $n_0 = -0.002146625$; $a_f = 0.915392$.

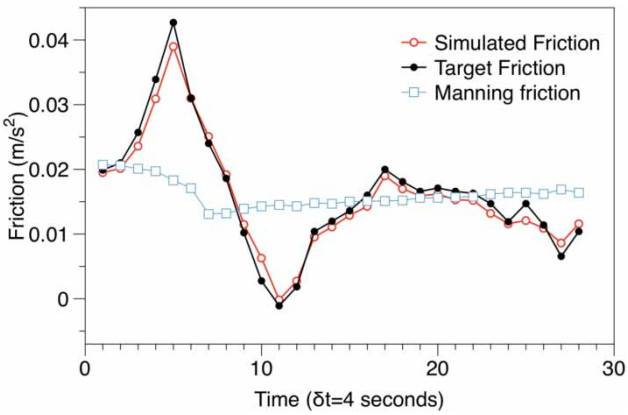

Figure 6 | Target friction, Manning friction, and simulated friction by proposed friction formula for Flood 1-2.

Validation of the proposed friction formula with Qiantang River flood data

The water level in Wenjianyan section can be calculated using the differential equation (Equation (14)) with measured water level and flow velocity in the upper section (Zhijiang section) as input. The differential model using the proposed friction formula can be tested by the comparisons between calculated and measured water level. Table 7 shows the simulation results of water level during the selected periods. The model was tested against the water level during both the wet and dry seasons. Event numbers 1–4 in Table 7 were selected for parameter calibration. The calibrated parameters n_0 and a_f are –0.0013008 and 0.8140032 respectively. For explanatory purposes, we plotted the observed and simulated water level graph of Wenjiayan section in Figure 7 during the period 2010-5-9 8:00 to 2010-5-13 7:00. The simulation results indicate that the differential model using the proposed friction formula can simulate the water level in the study location accurately. The water level is determined by complex interactions between tides and floods since Wenjiayan is located in the tidal reach. Traditional hydrodynamic models always present a poor performance in simulating the water level within a tidal reach (Bao *et al.* 2010). However, the proposed friction determination could improve the simulation of water levels in a tidal reach.

Table 7 | Simulation results of the water level (H) at Wenjiayan location

Number	Period	RE(H)
1	2009.11.1.8:00–2009.11.5.8:00	0.913
2	2009.11.5. 8:00–2009.12.1.8:00	0.988
3	2010.4.9.9:00–2010.4.16.9:00	0.977
4	2010.6.8.9:00–2010.7.1.8:00	0.787
5	2009.12.1.8:00–2009.12.30.8:00	0.974
6	2010.5.8.10:00–2010.6.7.7:00	0.872

CONCLUSION

In this study, the mechanism of friction was thoroughly analyzed. It was found that the Manning formula tends to simulate the friction with little variability, which contributes to large errors in the simulation of water level and flow

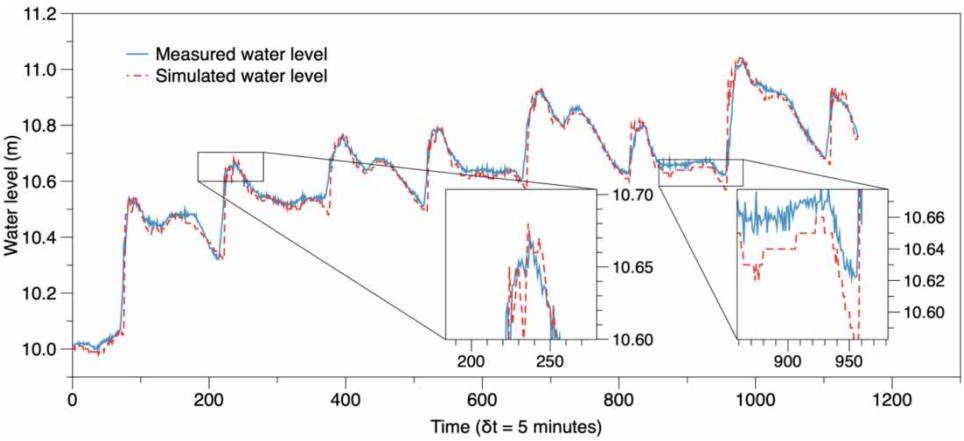

Figure 7 | Measured water level and simulated water level using the proposed friction formula in Wenjiayan location.

velocity. An improved friction formula is proposed based on the relationships between roughness coefficient and energy gradient in open-channel sections. Then, the differential model of one-dimensional flow was constructed based on the proposed friction formula. The improved friction formula was tested with both experimental flood data and the data from Qiantang River. The testing and simulation results can be summarized as below:

(1) The proposed friction formula provides a good simulation of target and the differential model using the proposed friction formula can simulate the water level and flow velocity well in both calibration and validation phases.
(2) The parameters in the proposed friction formula are less sensitive to the river section characteristics represented by different types of fences in this study than that of the Manning friction formula. In other words, the parameters in the proposed formula remain steadier than those in the Manning formula regarding different river section characteristics. In practice, the characteristics of the river section are extremely complex and may change along the river. The determination of parameters could be very difficult. If the parameters are relatively stable, we could use the same set of parameters for all river sections with different characteristics and still provide reliable simulations. As a result, the proposed friction formula has strong adaptability.
(3) The differential model using the proposed friction formula can improve the simulation of water level in tidal reaches where the water level is hard to simulate due to the complex interactions between tides and floods. The water level forecasting in a tidal reach is among the most critical problems for flood management and flood control because the water level is impacted by the interaction of upper reach flood wave and downstream tide wave (Qu *et al.* 2009). The calibrated differential model using the proposed friction formula could be used as a tool for water level forecasting in tidal reaches.

ACKNOWLEDGEMENTS

This study was supported by the National Natural Science Foundation of China (Grant Nos. 51279057 and 41371048), the Fundamental Research Funds for the Central Universities (Grant No. 2014B35314), Ministry of water resources public welfare industry special scientific research Project (Grant No. 201401034), Major Program of National Natural Science Foundation of China (Grant Nos. 51190090 and 51190091), IWHR Research & Development Support Program (JZ0145B012019), and the Open Research Fund Program of State Key Laboratory of Hydrology-Water Resources and Hydraulic Engineering (2015490611).

REFERENCES

Arcement, G. J. & Schneider, V. R. 1989 *Guide for Selecting Manning's Roughness Coefficients for Natural Channels and Flood Plains*. US Government Printing Office, Washington, DC, USA.

Bao, W., Zhang, X. & Qu, S. 2009 Dynamic correction of roughness in the hydrodynamic model. *J. Hydrodynam. B* **21** (2), 255–263.

Bao, W., Zhang, X., Yu, Z. & Qu, S. 2010 Real-time equivalent conversion correction on river stage forecasting with Manning's formula. *J. Hydrol. Eng.* **16** (1), 1–9.

Bathurst, J. C. 1985 Flow resistance estimation in mountain rivers. *J. Hydraul. Eng.* **111** (4), 625–643.

Chow, V. T., Maidment, D. R. & Mays, L. W. 1988 *Applied Hydrology*. McGraw-Hill, Singapore.

Darcy, H. & Bazin, H. 1865 *Hydraulic Research*. Dunod, Paris (in French).

De Doncker, L., Troch, P., Verhoeven, R., Bal, K., Meire, P. & Quintelier, J. 2009 Determination of the Manning roughness coefficient influenced by vegetation in the river Aa and Biebrza river. *Environ. Fluid Mech.* **9** (5), 549–567.

Dong, W.-J. & Yang, Z.-S. 2002 Calculation method for inverse problem of 1-D St. Venant equations. *J. Hydraul. Eng.* **33** (9), 61–65.

Dou, G. 1982 The general rule of laminar flow and turbulent flow in open channel and pipeline. *Sci. China Press* **A** (5), 472–480 (in Chinese).

Du Buat, P. 1822 *Chevalier Du Buat's Principles of Hydraulics*, translated by TF De Havilland, Vol. 2. Asylum Press, Madras.

Eytelwein, J. A. 1826 *Handbook of Hydrostatics*. Nabu Press, Berlin.

Grant, W. D. & Madsen, O. S. 1982 Movable bed roughness in unsteady oscillatory flow. *J. Geophys. Res. Oceans (1978–2012)* **87** (C1), 469–481.

Herschel, C. 1897 On the origin of the Chézy formula. *J. Assoc. Eng. Soc.* **18**, 363–369.

Ikeda, S., Parker, G. & Sawai, K. 1981 Bend theory of river meanders. Part 1. Linear development. *J. Fluid Mech.* **112**, 363–377.

Jones, O. 1976 An improvement in the calculation of turbulent friction in rectangular ducts. *J. Fluids Eng.* **98** (2), 173–180.

Khatibi, R. H., Williams, J. J. & Wormleaton, P. R. 2000 Friction parameters for flows in nearly flat tidal channels. *J. Hydraul. Eng.* **126** (10), 741–749.

Li, Z.-W. & Fang, C.-M. 2010 Energy dissipation law of bend flow and its implication. *J. China Inst. Water Resour. Hydropower Res.* **3**, 13.

Limerinos, J. T. 1970 *Determination of the Manning Coefficient From Measured Bed Roughness in Natural Channels*. Water Supply paper 1898-B. U.S. Geological Survey, Washington, DC.

McLaren, P. & Bowles, D. 1985 The effects of sediment transport on grain-size distributions. *J. Sediment. Res.* **55** (4), 457–470.

Murillo, J. & García-Navarro, P. 2014 Accurate numerical modeling of 1D flow in channels with arbitrary shape. Application of the energy balanced property. *J. Comput. Phys.* **260**, 222–248.

Nanson, G. C. & Knighton, A. D. 1996 Anabranching rivers: their cause, character and classification. *Earth Surf. Process. Landf.* **21** (3), 217–239.

Pannone, M., De Vincenzo, A. & Brancati, F. 2013 A mathematical model for the flow resistance and the related hydrodynamic dispersion induced by river dunes. *J. Appl. Math.* **2013**, 1–9.

Qi, W., Cao, W., Zhang, Y. & Guo, Q. 2013 Critical flow energy loss of sedimentation equilibrium of Lower Yellow River. *J. Sediment Res.* **5**, 15–20.

Qu, S., Wei-min, B., Peng, S., Zhongbo, Y. & Peng, J. 2009 Water-stage forecasting in a multitributary tidal river using a bidirectional Muskingum method. *J. Hydrol. Eng.* **14** (12), 1299–1308.

Willcocks, S. W. & Holt, R. 1899 *Elementary Hydraulics*. National Printing Office, Cairo.

Xiekang, W., Duo, F. & Shuyou, C. 2000 Experimental study on characteristics of roughness in the natural river. *J. Hydroelec. Eng.* **2**, 49–55 (in Chinese).

Yang, C. T. 1972 Unit stream power and sediment transport. *J. Hydr. Div. ASCE.* **98** (HY10), 1805–1825.

Yang, K., Cao, S. & Liu, X. 2007 Flow resistance and its prediction methods in compound channels. *Acta Mech. Sinica* **23** (1), 23–31.

Yao, W.-Y., Zheng, Y.-S. & Zhang, M. 2010 Discussion on the mechanism of river meandering. *Adv. Water Sci.* **21** (4), 533–540.

Yen, B. C. 2002 Open channel flow resistance. *J. Hydraul. Eng.* **128** (1), 20–39.

Zhao, L. & Zhang, H. 1997 Study of flow frictional characteristics in the Lower Yellow River channel. *Yellow River* **9**, 1–5 (in Chinese).

First received 20 March 2019; accepted in revised form 29 July 2019. Available online 3 September 2019